Hierarchical Long-Term and Short-Term Production Optimization

G.M. van Essen, SPE, and **P.M.J. Van den Hof,** Delft University of Technology; and **J.D. Jansen,** SPE, Delft University of Technology and Shell

Summary

Model-based dynamic optimization of oil production has a significant potential to improve economic life-cycle performance, as has been shown in various studies. However, within these studies, short-term operational objectives are generally neglected. As a result, the optimized injection and production rates often result in a considerable decrease in short-term production performance. In reality, however, it is often these short-term objectives that dictate the course of the operational strategy. Incorporating short-term goals into the life-cycle optimization problem, therefore, is an essential step in model-based life-cycle optimization. We propose a hierarchical optimization structure with multiple objectives. Within this framework, the life-cycle performance in terms of net present value (NPV) serves as the primary objective and short-term operational performance is the secondary objective, such that optimality of the primary objective constrains the secondary optimization problem. This requires that optimality of the primary objective does not fix all degrees of freedom (DOF) of the decision variable space. Fortunately, the life-cycle optimization problem is generally ill-posed and contains many more decision variables than necessary. We present a method that identifies the redundant DOF in the life-cycle optimization problem, which can subsequently be used in the secondary optimization problem. In our study, we used a 3D reservoir in a fluvial depositional environment with a production life of 7 years. The primary objective is undiscounted NPV, while the secondary objective is aimed at maximizing short-term production. The optimal life-cycle waterflooding strategy that includes short-term performance is compared to the optimal strategy that disregards short-term performance. The experiment shows a very large increase in short-term production, boosting first-year production by a factor of 2, without significantly compromising optimality of the primary objective, showing a slight drop in NPV of only –0.3%. Our method to determine the redundant DOF in the primary objective function relies on the computation of the Hessian matrix of the objective function with respect to the control variables. Although theoretically rigorous, this method is computationally infeasible for realistically sized problems. Therefore, we also developed a second, more pragmatic, method relying on an alternating sequence of optimizing the primary- and secondary-objective functions. Subsequently, we demonstrated that both methods lead to nearly identical results, which offers scope for application of hierarchical long-term and short-term production optimization to realistically sized flooding-optimization problems.

Introduction

In recent years, improvements in dynamic reservoir modeling and measurement and control capabilities have lead to an increased interest in model-based operation of oil fields. Several studies have shown that there may be a significant scope for improving reservoir management by using reservoir models to optimize economic life-cycle performance [see, for example, Asheim (1988), Sudaryanto and Yortsos (2000), Brouwer and Jansen (2004), and Sarma et al. (2005)]. Especially combined with methods to reduce uncertainty—referred to as closed-loop reservoir management [see, for example, Nævdal et al. (2006), Sarma et al. (2008), Chen et al. (2009), Jansen et al. (2009), and Wang et al. (2009)]—these (proactive) life-cycle optimization techniques seem to be promising alternatives to more-reactive approaches, which are current practice.

However, in these studies on improved life-cycle performance, the importance of meeting short-term targets (e.g., maximizing revenues over a short time interval) is generally neglected. As a result, many of the improvements in life-cycle performance are obtained at the expense of short-term objectives. In reality, however, it is often these short-term objectives that dictate the course of the operational strategy, especially in view of geological and economic uncertainties. Incorporating short-term goals into the life-cycle optimization problem, therefore, is an essential step in the route toward implementation of the closed-loop reservoir-management concept. To this end, Saputelli et al. (2005, 2006) proposed a multilevel hierarchical control structure, where the separation of the levels was based on different time scales and objectives.

Jansen et al. (2009) observed that significantly different optimized waterflooding strategies result in nearly equal values in NPV. They concluded that the life-cycle optimization problem is ill-posed and contains many more control variables than necessary. As a result, there exist multiple solutions to the optimization problem, and different initial guesses of an input $\mathbf{u}$ may lead to different solution points in an optimal subset $\mathcal{S}$ of the decision variable space $\mathcal{U}$.

The goal of this paper is to present a hierarchical optimization framework that is able to address both short-term and long-term objectives in a consistent manner. Although this framework is generic in nature, the presented approach is aimed at maximizing an economic life-cycle objective, in terms of NPV, without disregarding short-term performance. The existence and nature of multiple solutions in the life-cycle optimization problem are investigated because they provide the possibility to improve short-term operational goals while aiming for economic life-cycle optimality.

Life-Cycle Optimization Problem

The life-cycle (i.e., long-term) optimization problem does not impose any particular choice of depletion or modeling technique. It only requires the existence of at least one decision variable and the model being capable of providing relatively reliable long-term predictions. However, in many case studies, waterflooding is selected as the depletion method for a number of reasons:

- It is a common recovery mechanism.
- A waterflooding strategy involves many decision variables.
- The flooding process can be modeled reasonably accurately over long distances and periods of time.
- There is generally a significant scope for improvement.

For these reasons, waterflooding is also adopted as the production process within this work. However, the mathematical formulation is kept generic as far as possible. Because of the transient nature of the saturation distribution in an oil-producing reservoir, dynamic optimization must be performed over the entire life of the reservoir to improve economic life-cycle performance. This optimization problem can be expressed by the following mathematical formulation:

$$\max_{\mathbf{u}_{1:K}} J\left(\mathbf{u}_{1:K}\right), \quad \text{(1)}$$

$$s.t. \quad \mathbf{g}_{k+1}\left(\mathbf{u}_k, \mathbf{x}_k, \mathbf{x}_{k+1}\right) = 0, \; k = 0, \ldots, K-1, \; \mathbf{x}_0 = \bar{\mathbf{x}}_0, \quad \text{(2)}$$

This paper (SPE 124332) was accepted for presentation at the SPE Annual Technical Conference and Exhibition, New Orleans, 4–7 October 2009, and revised for publication. Original manuscript received for review 2 November 2009. Revised manuscript received for review 11 March 2010. Paper peer approved 26 April 2010.

$$\mathbf{c}_{k+1}\left(\mathbf{u}_{k+1},\mathbf{x}_{k+1}\right)\le\mathbf{0},\quad k=0,\ldots,K-1,\quad\ldots\ldots\ldots\ldots\ldots\ldots(3)$$

where $\mathbf{u}$ is the control vector (input vector), $\mathbf{x}$ is the state vector (gridblock pressures and saturations), $\mathbf{g}$ is a vector-valued function that represents the system equations, $\mathbf{x}_0$ is a vector of the initial conditions of the reservoir with prescribed value $\bar{\mathbf{x}}_0$, the subscript k indicates discrete time, and K is the total number of timesteps. A colon in a subscript indicates a range [e.g., $\mathbf{u}_{1:K}=\left(\mathbf{u}_1,\mathbf{u}_2,\ldots,\mathbf{u}_K\right)$. The vector of inequality constraints $\mathbf{c}$ relates to the capacity limitations of the wells. The objective function J is of an economic type, generally NPV:

$$J=\sum_{k=1}^{K}\left(\frac{\left\{\begin{array}{l}\displaystyle\sum_{i=1}^{N_{\text{inj}}}r_{wi}\cdot\left(u_{wi,i}\right)_k\\ \displaystyle+\sum_{j=1}^{N_{\text{prod}}}\left[r_{wp}\cdot\left(y_{wp,j}\right)_k+r_o\cdot\left(y_{o,j}\right)_k\right]\end{array}\right\}}{(1+b)^{\frac{t_k}{\tau_t}}}\cdot\Delta t_k\right),\quad\ldots\ldots\ldots(4)$$

where $u_{wi,i}$ is the control input representing the water-injection rate of Well i, $y_{wp,j}$ is the water-production rate of Well j, $y_{o,j}$ is the oil-production rate of Well j, r_{wi} is the water-injection costs (in USD/m^3), r_{wp} is the water-production costs (in USD/m^3), and r_o is the oil revenue (in USD/m^3), of which the latter three are assumed to be constant. Δt_k is the time interval of Timestep k in days. The term b represents the discount rate for a certain reference time τ_t. The terms N_{inj} and N_{prod} relate to the number of injection wells and production wells, respectively. In Eq. 4, the output variables $y_{wp,j}$ and $y_{o,j}$ relate to the water-production rate and oil-production rate of Well j, respectively, which form part of the output vector

$$\mathbf{y}_{k+1}=\mathbf{h}\left(\mathbf{u}_{k+1},\mathbf{x}_{k+1}\right),\quad k=0,\ldots,K-1,\quad\ldots\ldots\ldots\ldots\ldots\ldots(5)$$

with $\mathbf{h}$ a vector-valued output function that relates $\mathbf{y}$ to the control vector (input vector) $\mathbf{u}$ and the state $\mathbf{x}$. The term $u_{wi,i}$ represents those elements of $\mathbf{u}$ that involve the water-injection flow rates of Well i. An economic objective function such as Eq. 4 does not necessarily provide a unique solution to the optimization problem. Although it relates to realistic business conditions, it may well cause ill-posedness of the problem.

Several methods exist to attack the dynamic optimization problem of batch-like processes [see, for example, Srinivasan et al. (2003)]. However, the size of the waterflooding-optimization problem (Eqs. 1 through 3) limits the possibilities. Simultaneous methods or dynamic programming are impractical because of the usually very large number of states of reservoir models. The resulting long simulation times and large number of input variables also rule out search methods that require many function evaluations (e.g., genetic algorithms). A viable optimization technique is a gradient-based method using a set of adjoint equations to determine the gradients [see, for example, Brouwer and Jansen (2004), Sarma et al. (2005), and Kraaijevanger et al. (2007)]. This approach to life-cycle waterflooding optimization is encountered most often in literature and is also the method implemented in the proprietary reservoir simulator used in this study.

Hierarchical Optimization

Multiple Objectives. In the life-cycle waterflooding problem as expressed by Eqs. 1 through 3, the desire to aim for maximal short-term (daily) production is discarded. A balanced objective provides a possibility to address both objectives in a single function; see Marler and Arora (2004):

$$J_{\text{bal}}=\omega_1\cdot J_1+\omega_2\cdot J_2.\quad\ldots\ldots\ldots\ldots\ldots\ldots\ldots\ldots\ldots\ldots(6)$$

Here J_{bal} is the balanced objective function constructed from the weighted long-term and short-term objective functions J_1 and J_2. The terms ω_1 and ω_2 are weighting factors of the short- and long-term objective, respectively. In the economic objective function (Eq. 4) the discount rate b, apart from representing the time value of money, may also be used to weigh the importance of short-term against long-term performance. In that respect, the discount factor may also be seen as a weighting factor to balance the importance of multiple objectives. However, the difficulty in a balanced objective function lies in finding suitable weighting factors between the objectives. This is especially the case if the values of the multiple objective functions have different physical interpretations. Because the weighting factors strongly determine the characteristics of the optimal solution, a large number of trial-and-error runs with different weighting factors may be required to obtain a satisfactory one.

As an alternative, we propose a hierarchical optimization structure—sometimes referred to as the lexicographic method—that requires a prioritization of the multiple objectives, as described in Haimes and Li (1988). In this structure, optimization of a secondary objective function J_2 is constrained by the requirement that the primary objective function J_1 must remain close to its optimal value J_1^*. This structure can be expressed mathematically as

$$\max_{\mathbf{u}_{1:K}}J_2\left(\mathbf{u}_{1:K}\right),\quad\ldots\ldots\ldots\ldots\ldots\ldots\ldots\ldots\ldots\ldots\ldots\ldots(7)$$

$$s.t.\quad\mathbf{g}_{k+1}\left(\mathbf{u}_k,\mathbf{x}_k,\mathbf{x}_{k+1}\right)=0,\ k=0,\ldots,K-1,\ \mathbf{x}_0=\bar{\mathbf{x}}_0,\quad\ldots\ldots(8)$$

$$\mathbf{c}_{k+1}\left(\mathbf{u}_{k+1},\mathbf{x}_{k+1}\right)\le0,\quad k=0,\ldots,K-1,\quad\ldots\ldots\ldots\ldots\ldots\ldots(9)$$

$$J_1^*-J_1\left(\mathbf{u}_{k+1}\right)\le\varepsilon,\quad k=0,\ldots,K-1,\quad\ldots\ldots\ldots\ldots\ldots\ldots(10)$$

where ε is an arbitrary small value compared to J_1^*. Solving Eqs. 7 through 10 requires the knowledge of J_1^*, which is obtained through solving the optimization-problem equations (Eqs. 1 through 3). In the hierarchical optimization structure (Eqs. 7 through 10), the optimum value of the life-cycle objective function J_1 constrains optimization of the short-term objective. It should be noted that this ordering of long and short term by no means is unique. Alternatively, one may want to optimize life-cycle performance under the condition that certain short-term production targets are met. In that case, the short-term goals act as constraints on the life-cycle optimization problem.

Redundant DOFs. Jansen et al. (2009) described that different solutions exist for the optimal control problem of maximizing an economic objective function over the life of the reservoir. The existence of multiple solutions was attributed to the ill-posedness of the optimal control problem. The ill-posedness also suggests that, even when optimality of an economic life-cycle objective is reached, not all DOFs of the decision variable space $\mathcal{U}$ are fixed and not all solution points in the optimal subset $\mathcal{S}$ are connected. This means that there may exist redundant DOFs in the optimization problem. Huesman et al. (2007, 2008) found similar results for economic dynamic optimization of plantwide operation. A consequence of these redundant DOFs is that, even if ε in Eq. 10 is chosen equal to 0, DOFs are left to improve the secondary objective function J_2. A straightforward way of investigating this is to imbed Eq. 10 as an equality constraint in the adjoint formulation by means of an additional Lagrange multiplier. Unfortunately, the adjoint functionality in the simulator used in our study was not yet capable of dealing with (additional) state constraints. Alternatively, unconstrained gradient information can be used to investigate the redundant DOFs, as described in the next section.

Quadratic Approximation of the Objective Function. In the following, we will use the short-cut notation $\mathbf{u}$ to indicate the input sequence $\mathbf{u}_{1:K}=\left(\mathbf{u}_1,\mathbf{u}_2,\ldots,\mathbf{u}_K\right)$. A solution $\mathbf{u}$ for which no constraints are active is an optimal solution $\mathbf{u}^*$ if and only if the gradients of J with respect to $\mathbf{u}$ are zero [i.e., $(\partial J/\partial\mathbf{u})^T=0$]. As a result, at $\mathbf{u}^*$, the gradients do not provide any information on possible redundant DOFs under the optimality condition on J. Second-order derivatives of J with respect to $\mathbf{u}$ are collected in the Hessian matrix $\mathbf{H}=\partial^2J/\partial\mathbf{u}^2$. If $\mathbf{H}$ is negative definite, the considered solution $\mathbf{u}$ is an optimal solution, but no DOFs are left when the optimality condition on J holds. If $\mathbf{H}$ is negative semidefinite,

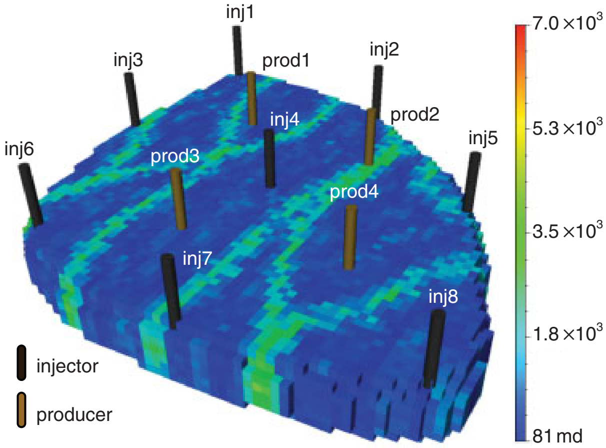

Fig. 1—3D oil-reservoir model (Van Essen et al. 2009).

the Hessian does not have full rank. An orthonormal basis **B** for the undetermined directions of **H** can then obtained through a singular value decomposition:

$$\mathbf{H} = \mathbf{U}\mathbf{\Sigma}\mathbf{V}^T. \quad (11)$$

The orthonormal basis **B** consists of those columns of **V** that relate to singular values of zero; i.e.

$$\mathbf{B} \triangleq \left(\mathbf{v}_i \middle| \sigma_i = 0, \quad i = 1,\ldots,N_\mathbf{u}\right), \quad (12)$$

where $\mathbf{v}_i$ is the ith column of **V**, σ_i is the ith singular value, and $N_\mathbf{u}$ is the number of DOFs in the input. Note that, because of the symmetrical nature of the Hessian matrix **H**, the singular value decomposition may be replaced by a computationally more efficient eigenvalue decomposition, in which case the eigenvectors relating to eigenvalues equal to zero span the orthonormal basis **B**.

Not all orthogonal directions spanned by the columns of **B** will be redundant DOFs. These directions are redundant DOFs if they are linear and if all higher-order derivatives are zero also, which, at this point in time, is impossible to prove for reservoir models. **B**, however, is a basis for redundant DOFs for a quadratic approximation $\hat{J}$ of objective function J. Because $\hat{J}$ can be considered to be an acceptable approximation for small deviations from $\mathbf{u}^*$, **B** can be regarded as an acceptable basis for the redundant DOFs for small deviations from $\mathbf{u}^*$.

Approximate Hessian Matrix. Unfortunately, no reservoir-simulation package is currently capable of calculating second-order derivatives. However, using the gradient information, second-order derivatives can be approximated. In our study, we used a forward-difference scheme:

$$\frac{\partial^2 J}{\partial u_i \partial u_j} \approx \frac{\nabla J_i\left(\mathbf{u}+h_j\mathbf{e}_j\right)-\nabla J_i\left(\mathbf{u}\right)}{2h_j} + \frac{\nabla J_j\left(\mathbf{u}+h_i\mathbf{e}_i\right)-\nabla J_j\left(\mathbf{u}\right)}{2h_i}, \quad (13)$$

where ∇J_i is the ith element of the gradient $\nabla J = \left(\partial J/\partial \mathbf{u}\right)^T$, $\mathbf{e}_i$ is a canonical unit vector (i.e., a vector with a 1 at element i and 0 elsewhere), and h_i is the perturbation step size that relates to parameter $\mathbf{u}_i$ of $\mathbf{u}$. In total, $N_\mathbf{u}$+1 simulations (function evaluations) are required to obtain the approximate Hessian matrix $\hat{\mathbf{H}}$ at a particular optimal solution $\mathbf{u}^*$.

Alternatively, a reduced Hessian method could be used that approximates only that portion of the Hessian relevant for the subspace in which the Hessian is negative (or positive) definite; see Byrd and Nocedal (1990). If the Hessian is negative (or positive) semidefinite, the tangent space of this subspace will be equal to the null space of the complete Hessian matrix. This could lead to a significant reduction in computational burden, especially when the dimensions of the null space are large.

TABLE 1—GEOLOGICAL AND FLUID PROPERTIES FOR EXAMPLE

Property	Value	Units
ϕ	0.20	–
ρ_o (at1 bar)	900	kg/m^3
ρ_w (at 1 bar)	1000	kg/m^3
c_o	1×10^{-5}	1/bar
c_w	1×10^{-5}	1/bar
μ_o	5×10^{-3}	Pa·s
μ_w	1×10^{-3}	Pa·s
p_{cow}	0	bar

Hierarchical Optimization Method. Adopting the approximation of H as described in the preceding subsection, the following iterative procedure is proposed to attack the hierarchical optimization problem (Eqs. 7 through 10) with $\varepsilon = 0$:

(1) Find a (single) optimal strategy $\mathbf{u}^*$ that maximizes the primary objective function J_1 and use $\mathbf{u}_n = \mathbf{u}^*$, with $n = 0$, as a starting point in the secondary optimization problem, where n is the iteration index.

(2) Approximate the Hessian matrix **H** of J_1 with respect to the input variables at (initial input) $\mathbf{u}_n$, and determine an orthonormal basis **B** for the null space of $\hat{\mathbf{H}}$.

(3) Find the improving direction **s** for the secondary objective function J_2 (e.g., the gradients $\partial J_2/\partial \mathbf{u}_n$).

(4) Project **s** onto the orthonormal basis **B** to obtain projected direction **d**, such that **d** is an improving direction for J_2 but does not affect J_1. The projection is performed using projection matrix **P** according to

$$\mathbf{d} = \mathbf{P} \cdot \mathbf{s}^T, \quad (14)$$

$$\mathbf{P} = \mathbf{B}\mathbf{B}^T. \quad (15)$$

(5) Update $\mathbf{u}_n$ using projected direction **d** in a steepest-ascent method,

$$\mathbf{u}_{n+1} = \mathbf{u}_n + \tau \cdot \mathbf{d}, \quad (16)$$

where τ is an appropriately small step size such that the quadratic approximation of J_1 is justified.

(6) Perform Steps 2 through 5 until convergence of J_2.

Note that, for the improving direction **s** for secondary objective function J_2, alternatives exist besides the steepest-ascent direction $\partial J_2/\partial \mathbf{u}$ (e.g., using a quasi-Newton or conjugate gradient method). This does not change the steps of the hierarchical optimization method but may speed up convergence of the procedure. In the next section, a numerical example will be presented in which the iterative hierarchical optimization structure is tested on a 3D heterogeneous reservoir model.

Example

We applied the hierarchical optimization procedure to a 3D oil-reservoir model, introduced in Van Essen et al. (2009). The life cycle of the reservoir covers a period of 3,600 days. The reservoir model consists of 18,553 gridblocks, as depicted in **Fig. 1,** and has dimensions of 480×480×28 m. Its geological structure involves a network of fossilized meandering channels. The average reservoir pressure is 400 bar. All remaining geological and fluid properties used in this example are presented in **Table 1.**

The reservoir model contains eight injection wells and four production wells. The production wells are modeled using a standard

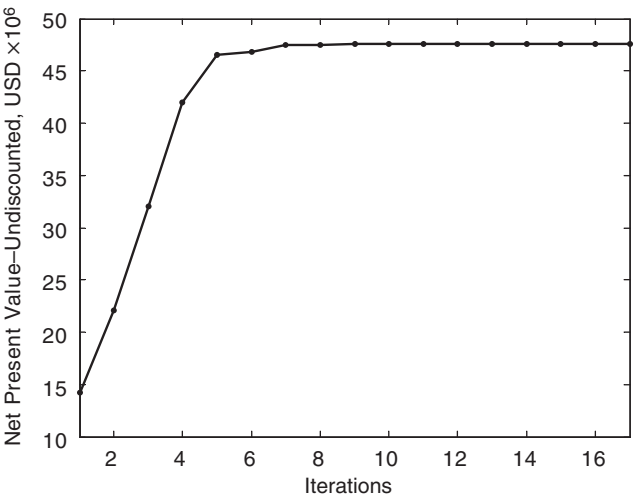

Fig. 2—Plot of the value of the objective function (NPV) against the iteration number of the life-cycle optimization problem. The iterations of the line-search algorithm are not shown in this plot.

Peaceman well model, which relates the source (output) term **y** to the difference between the well pressure and gridblock pressure:

$$y_k^j = w_j \cdot \left(p_{wf,k}^j - p_k^j\right), \quad \ldots\ldots\ldots\ldots\ldots\ldots\ldots\ldots\ldots\ldots (17)$$

where p_{wf} is the flowing wellbore pressure (bottomhole pressure), j is the index of the gridblock containing the well, and p_k^j is the pressure of the gridblock in which the well is located. The well index w_j is a constant, which contains the well's geometric factors and the rock and fluid properties of the reservoir directly around the well. The wells operate at a constant bottomhole pressure p_{wf} of 395 bar. The flow rates of the injection wells can be manipulated directly (i.e., the control input **u** involves injection flow-rate trajectories for each of the eight injection wells). The minimum rate for each injection well is 0.0 m^3/d; the maximum rate is set at 79.5 m^3/d. The control input **u** is reparameterized in time using a zero-order-hold scheme with input parameter vector θ. For each of the eight injection wells, the control input **u** is reparameterized into four time periods t_θ of 900 days during which the injection rate is held constant at value θ_i. Thus, the input parameter vector θ consists of 8×4 = 32 elements.

Life-Cycle Optimization. The objective function for the life-cycle optimization was defined in terms of NPV, as defined in Eq. 4, with r_o = 126 USD/m^3, r_{wp} = 19 USD/m^3, and r_{wi} = 6 USD/m^3. The discount rate b was set to 0. Thus, the life-cycle objective relates to undiscounted cumulative cash flow. The optimal input—denoted by $\mathbf{u}_\theta^*$—was obtained using a steepest-ascent scheme together with a line-search algorithm. It was terminated after 17 iterations (excluding the iterations of the line search) when the line-search algorithm was not able to find a significant improvement in NPV. Convergence to the optimal solution of the life-cycle optimization problem may be speeded up using a quasi-Newton or conjugate gradient method. However, as efficiency of the optimization algorithm was not the objective of this study, the more simplistic steepest-ascent scheme was used. The value of NPV against the iteration number can be observed in **Fig. 2.** The final optimal input $\mathbf{u}_\theta^*$ of the life-cycle optimization problem is shown in **Fig. 3.** Note that none of the input constraints (Eq. 9) is active for $\mathbf{u}_\theta^*$. The value of the objective function corresponding to input $\mathbf{u}_\theta^*$ is USD 47.6×10^6.

Hierarchical Optimization. In a realistic setting, short-term production optimization will be aimed at maximizing the oil production over the short time horizon of interest, while repeating this exercise as time goes by (i.e., using a moving-horizon approach). In view of the simplicity of the presented example, this short-term production objective, which involves successive reoptimization, is replaced by an objective that does not require reoptimization over the production life, while still emphasizing the importance of short-term production. Therefore, we chose the secondary objective J_2 to be identical to the primary objective function but with the addition of a very high annual discount rate b of 0.25. As a result, short-term production is weighed much more heavily than future production. However, as stated before, the particular choice of primary and secondary objective has no effect on the hierarchical procedure itself. Note that, because of the very high discount

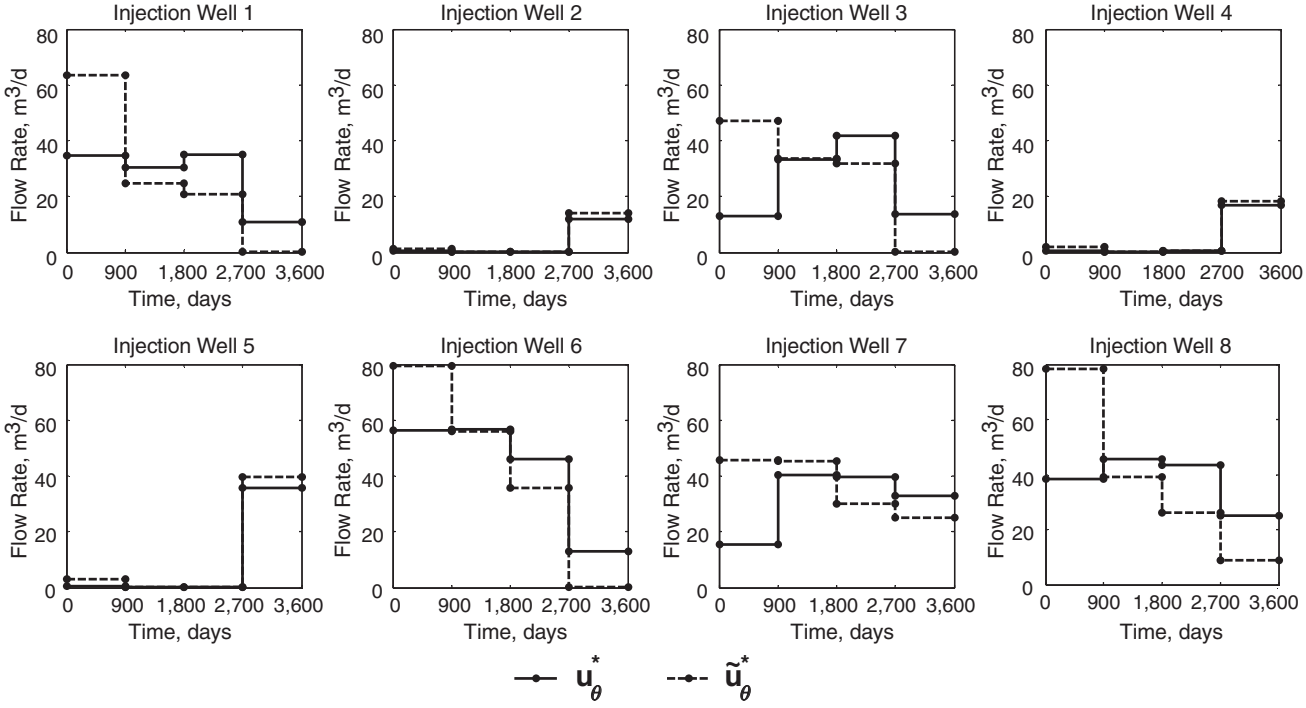

Fig. 3—Input trajectories for each of the eight injection wells for the initial optimal solution $\mathbf{u}_\theta^*$ to J_1 (solid line) and the optimal solution $\tilde{\mathbf{u}}_\theta^*$ after the constrained optimization of J_2 (dashed line).

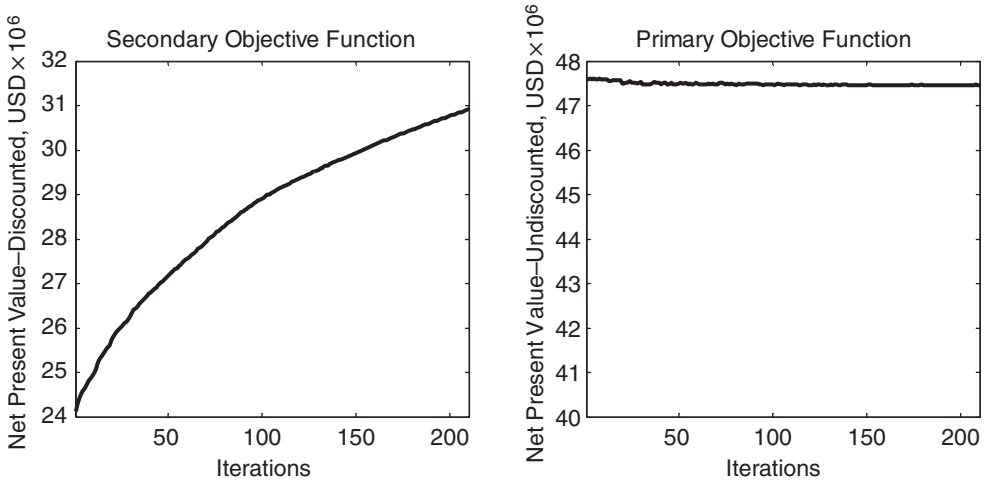

Fig. 4—Values of the secondary objective function J_2 and the primary objective function J_1 plotted against the iteration number for the constrained secondary optimization problem.

rate, the actual value of J_2 no longer has a realistic meaning in an economic sense.

Next, we applied the hierarchical approach as presented in the preceding subsection. The total number of simulation runs needed to approximate the Hessian ($\hat{\mathbf{H}}$) was 33, but the overall simulation time was kept within acceptable limits by parallel processing the simulations. Because this example involves a numerical model and an approximation of the second-order derivatives, we relaxed the selection criterion for $\mathbf{B}$. Those columns $\mathbf{v}_i$ of $\mathbf{V}$ were selected that correspond to singular values for which $\sigma_i/\sigma_1 < 0.02$ instead of $\sigma_i = 0$. The projected gradients $\mathbf{d}$ were again used in a steepest-ascent scheme. In order to ensure that $\mathbf{u}_{\theta,n+1}$ remains close to $\mathbf{u}_{\theta,n}$, $\mathbf{d}$ was normalized by dividing $\mathbf{d}$ by its largest absolute element. A step size τ of 1 was used in the steepest-ascent scheme, such that the largest update in the water-injection rates remained equal to 1. Through trial-and-error, this step size was considered appropriately small such that the quadratic approximation of J_1 was justified. The step size was kept constant during execution of the hierarchical optimization procedure because no downscaling was required to find an improving control input for J_2. Because of computing time restrictions, the hierarchical optimization of J_2 was terminated after 210 iterations, with final control input $\tilde{\mathbf{u}}_\theta^*$. The relatively slow convergence was because of the small step size required to allow for the quadratic approximation of J_1, but convergence may improve when a better improving direction for J_2 is used. At the start of the hierarchical optimization, the number of redundant DOFs was equal to 19, out of a total of 32 DOFs. During the 210 iterations, this number remained more or less constant.

To evaluate the results of the hierarchical optimization, the optimization of J_2 was also performed without projection on $\mathbf{B}$. As a result, the obtained control input—denoted by $\tilde{\mathbf{u}}_\theta$—in that case does not ensure optimality of J_1. **Fig. 4** displays the values of J_1 and J_2 plotted against the iteration number for the hierarchical optimization problem. It shows a considerable increase of J_2 of 28.2% and a slight drop of J_1 of –0.3%. In Fig. 3, the input strategy after the final iteration step is presented. It can be observed that the injection strategy shows a substantial increase in injection rates at the beginning of the production life and a decrease at the end.

As a comparison, we repeated the optimization of J_2 starting from $\mathbf{u}_\theta^*$ with the difference that it was no longer constrained by the requirement that J_1 remain close to J_1^* (i.e., Eq. 10 was omitted). The optimization procedure was terminated after 107 iterations when the improvement of J_2 was equal to 28.2% (i.e., the final value of J_2 in the constrained optimization case). The values of J_1 and J_2 plotted against the iteration number for the unconstrained optimization of J_2 are shown in **Fig. 5.** Again an increase in J_2 of 28.2% is realized, but now at a cost of a decrease in J_1 of –5.0%. Finally, **Fig. 6** shows the value of the primary objective function J_1 over time until the end of the producing reservoir life for $\mathbf{u}_\theta^*$, $\tilde{\mathbf{u}}_\theta^*$, and $\tilde{\mathbf{u}}_\theta$. Input $\tilde{\mathbf{u}}_\theta^*$ shows a steeper ascent of J_1 than $\mathbf{u}_\theta^*$, while their final values are nearly equal. Input $\tilde{\mathbf{u}}_\theta$ shows initially the same steep ascent, but J_1 drops toward the end of the life of the reservoir.

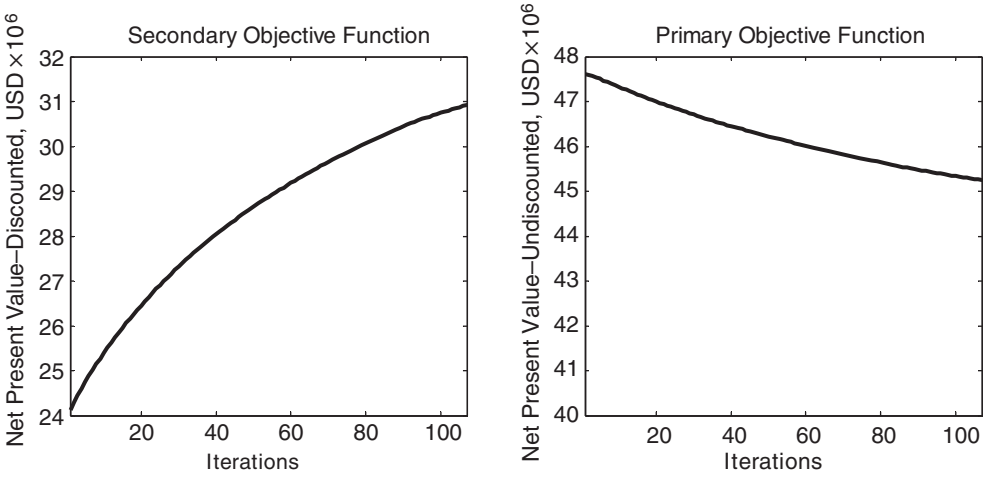

Fig. 5—Values of the secondary objective function J_2 and the primary objective function J_1 plotted against the iteration number for the secondary optimization problem, no longer constrained by the orthonormal basis B.

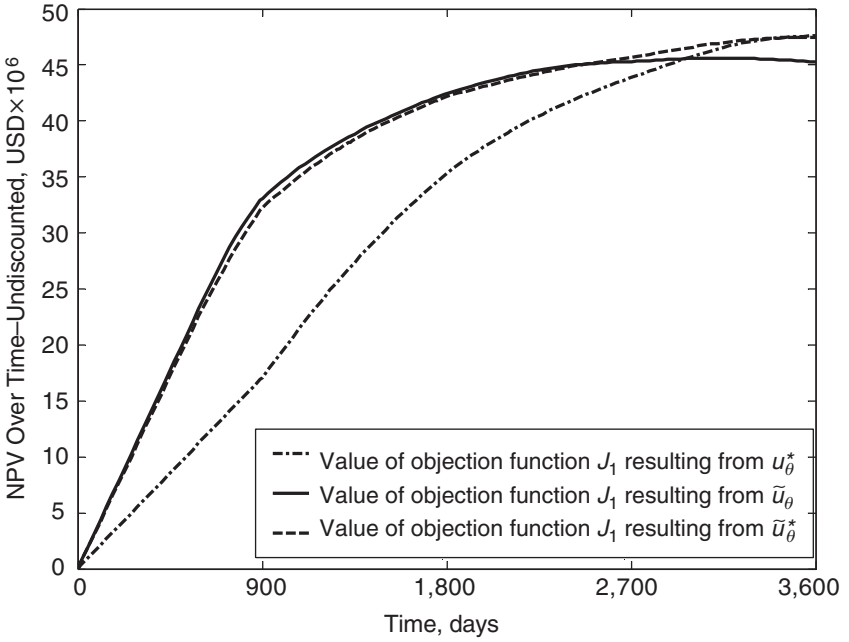

Fig. 6—Value of the primary objective function J_1 over time for initial optimal input $\mathbf{u}_\theta^\star$ to J_1 (dashed/dotted line), the optimal input $\tilde{\mathbf{u}}_\theta^\star$ after the constrained optimization of J_2 (dashed line), and input $\tilde{\mathbf{u}}_\theta$ after the unconstrained optimization of J_2 (solid line).

Alternative Methods

The presented hierarchical optimization approach is computationally very demanding and becomes infeasible for more-realistic reservoir models with an increased number of input parameters, even when reduced-Hessian techniques are used. It should be noted, however, that execution of the hierarchical optimization procedure does not require knowledge of all redundant DOFs explicitly. In theory, the inequality constraint (Eq. 10) could be incorporated in the adjoint formulation through the use of an additional Lagrange multiplier, by which the calculation of second-order derivatives is avoided altogether. However, this would require modifications to the reservoir simulator, and, therefore, we did not pursue this route. An alternative method to solve the hierarchical optimization problem without explicitly calculating the redundant DOFs is through the use of a balanced objective function as described by Eq. 6, with the variation of using weighting functions Ω_1 and Ω_2 instead of weighting factors ω_1 and ω_2:

$$J_{\text{bal}} = \Omega_1 \cdot J_1 + \Omega_2 \cdot J_2, \quad \ldots\ldots\ldots\ldots\ldots\ldots\ldots\ldots\ldots\ldots (18)$$

where Ω_1 and Ω_2 are switching functions of J_1 and J_1^* that take on values of 1 and 0 or vice versa:

$$\Omega_1(J_1) = \begin{cases} 1 & \text{if } J^* - J_1 > \varepsilon \\ 0 & \text{if } J^* - J_1 \le \varepsilon \end{cases},$$
$$\Omega_2(J_1) = \begin{cases} 0 & \text{if } J^* - J_1 > \varepsilon \\ 1 & \text{if } J^* - J_1 \le \varepsilon \end{cases}. \quad \ldots\ldots\ldots\ldots\ldots\ldots\ldots\ldots\ldots\ldots (19)$$

Here, ε is the threshold value as defined in the inequality constraint (Eq. 10). The gradient of J_{bal} with respect to the input parameters $\mathbf{u}$ for iteration n+1 is then simply

$$\left.\frac{\partial J_{\text{bal}}}{\partial \mathbf{u}}\right|_{n+1} = \Omega_1(J_{1,n}) \cdot \left.\frac{\partial J_1}{\partial \mathbf{u}}\right|_{n+1} + \Omega_2(J_{1,n}) \cdot \left.\frac{\partial J_2}{\partial \mathbf{u}}\right|_{n+1}. \quad \ldots\ldots\ldots\ldots (20)$$

Execution of the optimization problem using balanced objective function (Eq. 18) sequentially gives improving directions for either J_1 or J_2. With each iteration, the value of J_2 either increases while the value of J_1 decreases or vice versa, as the solution moves to and from the feasible region with respect to the inequality constraint (Eq. 10). When no redundant DOFs are available, the control input would jump between two fixed solutions, of which only one would be feasible. However, in the case where redundant DOFs do exist, improvement of J_2 is possible without compromising Eq. 10 and convergence of the hierarchical optimization will occur in a zigzag fashion, as schematically represented in **Fig. 7.**

This switching method has the advantage that numerous evaluations of the system and adjoint equations are avoided: Only two runs (in parallel execution) of the system and adjoint equations are necessary per iteration, regardless of the number of input parameters. Second, the method is straightforward to implement. Finally, it provides the possibility to set a bound explicitly on the deviation of J_1 from J_1^* by choosing an appropriate value for ε. A disadvantage of the method is the slow convergence because of the infeasible solution steps. Also, some tuning of τ will be required to account for the fact that the Euclidean length of vectors $\partial J_1/\partial \mathbf{u}$ and $\partial J_2/\partial \mathbf{u}$ is different. As with the null-space approach, replacing the gradient vector $\partial J_2/\partial \mathbf{u}$ with an improving direction $\boldsymbol{s}$ for J_2 (obtained through, for example, a quasi-Newton or conjugate gradient method) may speed up convergence.

Example. The switching method was again applied to the 3D oil-reservoir model. Although the number of input parameters does not pose a problem to the switching method, again the control input was parameterized using 32 parameters to allow for a fair comparison with previous results. For the choice of threshold value ε, the maximum deviation of J_1 from J_1^* from the null-space method was used (–0.3%) (i.e., $\varepsilon = 0.997 \times J_1^*$). Just as in the null-space example, optimization of J_2 using the objective function (Eq. 18) was started from $\mathbf{u}_\theta^*$. The optimization procedure was again terminated when a feasible solution $\tilde{\mathbf{u}}_{\theta,sw}^*$ was found that gave an improvement of J_2 of 28.2%. The results of the hierarchical optimization problem using the switching method are shown in **Fig. 8.**

Fig. 8 shows that the switching method is able to give results for the hierarchical optimization problem similar to those of the null-space method, while requiring much fewer evaluations of the system and adjoint equations per iteration (2 vs. 33). The fact that the switching method also needs fewer iterations to reach the same level of improvement of J_2 is the result of better tuning of the algorithm's parameters and is not inherent to the method. In **Fig. 9** the feasible input strategy $\tilde{\mathbf{u}}_{\theta,sw}^*$ reached after the final iteration step of the switching method is presented, together with the initial input strategy $\mathbf{u}_\theta^*$ and the final input strategy $\tilde{\mathbf{u}}_\theta^*$ of the null-space method.

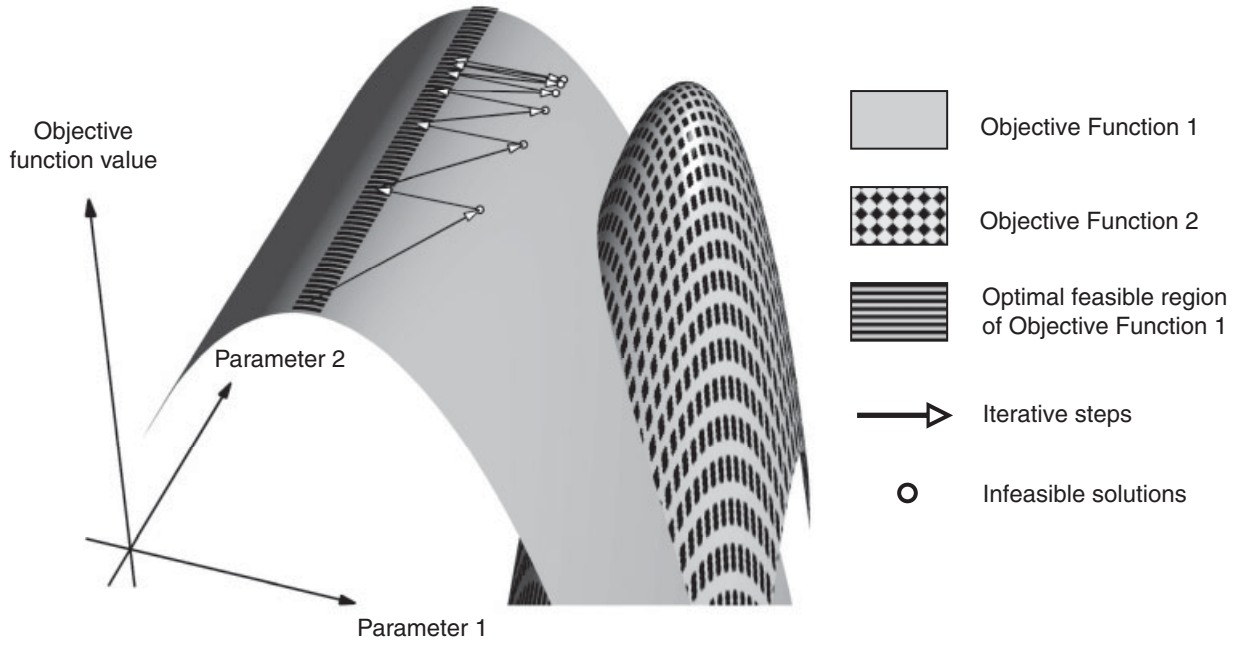

Fig. 7—Schematic representation of the iterative process of solving a hierarchical optimization problem using an objective function as described by Eqs. 18 and 19. The process converges toward a final solution in a zigzag fashion, moving into and out of the feasible region bounded by the optimal solutions of the primary objective function J_1.

Discussion and Conclusions

Discussion. In the hierarchical approach presented in this paper, long-term (life-cycle) recovery optimization was selected as the primary objective, while short-term production optimization served as the secondary objective. However, the concept of using the redundant DOFs of the primary objective to improve a secondary objective is not limited to this specific choice. Alternatively, the secondary objective function may be used, for example, to search for a smoother production profile, a bang/bang production profile [see Zandvliet et al. (2007)], or a persistently exciting production profile [see Zandvliet et al. (2008)]. Also, a different primary objective function may be chosen (e.g., ultimate recovery or short-term production), provided that it offers enough redundant DOFs to improve a secondary objective function.

In this paper, gradient information was used to prove the existence of redundant DOFs with respect to a life-cycle objective function. Moreover, gradients were at the heart of the presented null-space method to solve the hierarchical optimization problem. It should be noted, however, that there is no need to explicitly determine the null space using the gradients, as was shown using the switching method. Consequently, the optimization method used to attack the hierarchical optimization problem does not necessarily have to be gradient-based, which implies that alternative optimization methods (e.g., genetic algorithms) may also be considered.

Conclusions. We addressed the issue of multiple (long-term and short-term) objectives in oil-production optimization and investigated a hierarchical approach by means of a numerical experiment. On the basis of this experiment, we conclude that

- There exist redundant DOFs in the input strategy **u** with respect to the optimality of the long-term objective. This implies the existence of an optimal subset $\mathcal{S}$ of connected optimal solutions within the solution space $\mathcal{U}$.
- The redundant DOFs create enough freedom to improve a secondary, short-term objective function significantly. Moreover, the difference between the initial and final input strategy to the secondary optimization problem is substantial. This suggests that $\mathcal{S}$ occupies a considerable space within decision variable space $\mathcal{U}$.
- The presented hierarchical optimization procedure provides a method to incorporate short-term performance objectives into

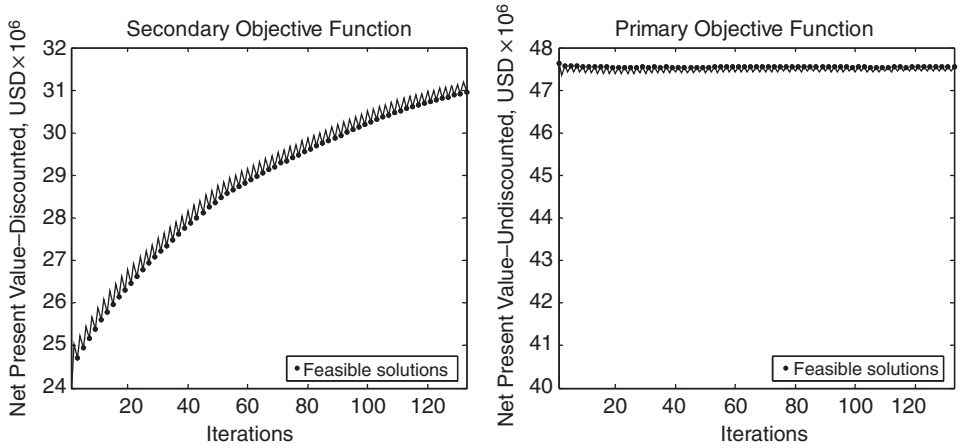

Fig. 8—Values of the secondary objective function J_2 and the primary objective function J_1 plotted against the iteration number for the secondary optimization problem, using the switching method. The "feasible solutions" marks relate to those solutions that are feasible with respect to the inequality constraint (Eq. 10).

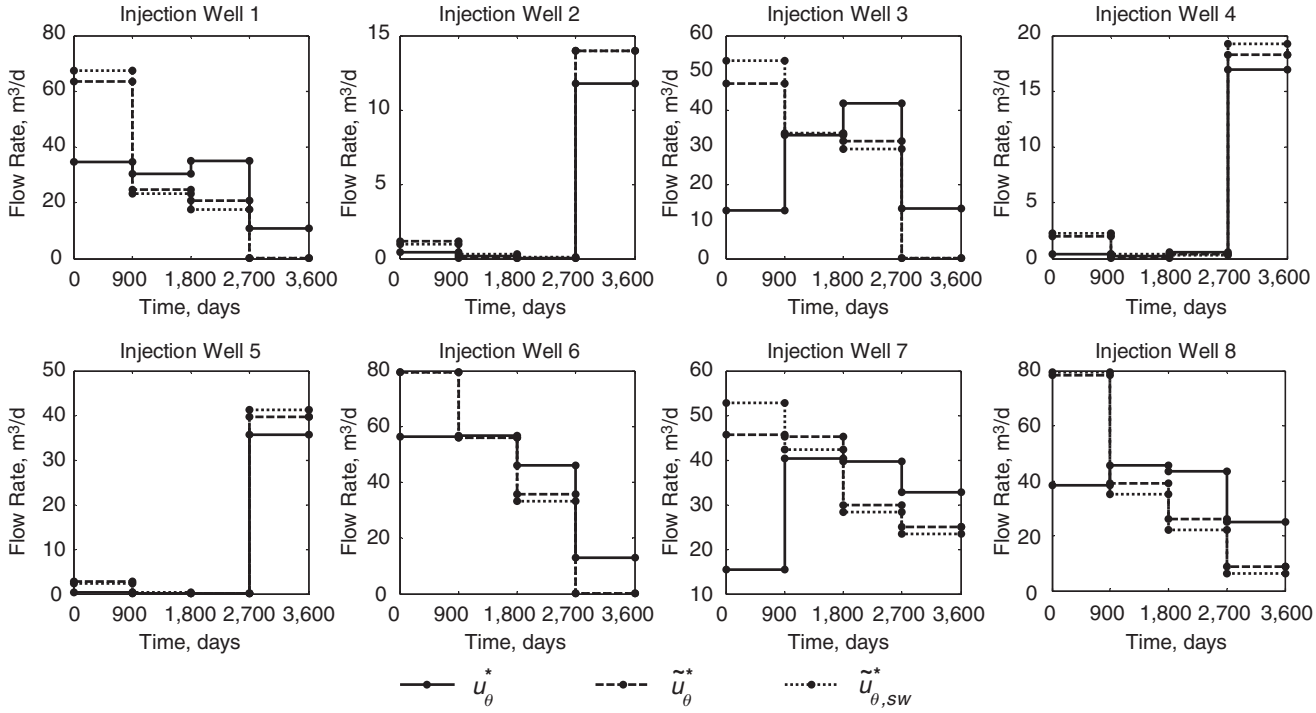

Fig. 9—Input trajectories for each of the eight injection wells for the initial optimal solution $\mathbf{u}^*_\theta$ to J_1 (solid line), the final solution $\tilde{\mathbf{u}}^*_\theta$ of the null-space method (dashed line), and the final solution $\tilde{\mathbf{u}}^*_{\theta,sw}$ of the switching method (dotted line).

the problem setting of maximizing life-cycle performance of oil recovery. Using the hierarchical structure, optimization of the secondary objective can be obtained without significantly compromising the primary objective.

- A theoretically rigorous method to select the redundant DOFs in the primary objective function requires computation of the Hessian of the objective function with respect to the control variables. This makes the theoretically rigorous method computationally too demanding for application to realistically sized problems.
- Nearly identical results can be obtained with the aid of a somewhat more pragmatic, but computationally much more efficient, switching method that, starting from an optimal long-term strategy, alternately optimizes the primary and secondary objective functions.

Nomenclature

b = discount rate
$\mathbf{B}$ = basis for redundant DOFs
c = compression
$\mathbf{d}$ = projected search direction on $\mathbf{B}$
$\mathbf{H}$ = Hessian matrix
$\hat{\mathbf{H}}$ = approximate Hessian matrix
J = objective function
$\hat{J}$ = second-order approximation of J
k = timestep counter
n = iteration index
p = pressure
$\mathbf{P}$ = projection matrix
r = revenues/costs
$\mathbf{s}$ = improving direction for J_2
S = saturation
t_k = time at Timestep k
$\mathbf{u}$ = input vector
$\mathbf{u}^*_\theta$ = optimal $\mathbf{u}$ for J_1
$\tilde{\mathbf{u}}^*_\theta$ = $\mathbf{u}$ optimized for J_2 constrained by $\mathbf{B}$
$\tilde{\mathbf{u}}_\theta$ = $\mathbf{u}$ optimized for J_2 not constrained by $\mathbf{B}$
w = well constant
$\mathbf{x}$ = state vector
$\bar{\mathbf{x}}_0$ = prescribed value of the initial condition
$\mathbf{y}$ = output vector
Δt_k = time interval of Timestep k
ε = tolerance of optimality constraint
μ = viscosity
τ = step size of algorithm
τ_t = reference time
ϕ = porosity
ω = weighting factor
Ω = weighting function
$\mathcal{S}$ = optimal subset of $\mathcal{U}$
$\mathcal{U}$ = decision variable space

Subscripts

cow = oil/water capillary
o = oil
wf = flowing wellbore
wi = injected water
wp = produced water
1 = primary
2 = secondary

Superscripts

* = optimal

Acknowledgments

This research was carried out within the context of the Integrated Systems Approach to Petroleum Production (ISAPP) knowledge center. ISAPP is a joint project between Delft University of Technology, Shell International Exploration & Production, and the Dutch Organization for Applied Scientific Research.

References

Asheim, H. 1988. Maximization of Water Sweep Efficiency by Controlling Production and Injection Rates. Paper SPE 18365 presented at the European Petroleum Conference, London, 16–19 October. doi: 10.2118/18365-MS.

Brouwer, D.R. and Jansen, J.-D. 2004. Dynamic Optmization of Water Flooding With Smart Wells Using Optimal Control Theory. *SPE J.* **9** (4): 391–402. SPE-78278-PA. doi: 10.2118/78278-PA.

Byrd, R.H. and Nocedal, J. 1990. An Analysis of Reduced Hessian Methods for Constrained Optimization. *Mathematical Programming* **49** (1–3): 285–323. doi: 10.1007/BF01588794.

Chen, Y., Oliver, D.S., and Zhang, D. 2009. Efficient Ensemble-Based Closed-Loop Production Optimization. *SPE J.* **14** (4): 634–645. SPE-112873-PA. doi: 10.2118/112873-PA.

Haimes, Y.Y. and Li, D. 1988. Hierarchical Multiobjective Analysis for Large-Scale Systems: Review and Current Status. *Automatica* **24** (1): 53–69. doi: 10.1016/0005-1098(88)90007-6.

Huesman, A.E.M., Bosgra, O.H. and Van den Hof, P.M.J. 2007. Degrees of Freedom Analysis of Economic Dynamic Optimal Plantwide Operation. *Proc.,* 8th International IFAC Symposium on Dynamics and Control of Process Systems, Cancún, Mexico, 6–8 June, Preprints Vol. 1, 165–170.

Huesman, A.E.M., Bosgra, O.H. and Van den Hof, P.M.J. 2008. Integrating MPC and RTO in the Process Industry by Economic Dynamic Lexicographic Optimization; An Open-Loop Exploration. Paper P123952 presented at the AIChE 2008 Annual Meeting, Philadelphia, Pennsylvania, USA, 16–21 November.

Jansen, J.D., Douma, S.D., Brouwer, D.R., Van den Hof, P.M.J., Bosgra, O.H., and Heemink, A.W. 2009. Closed Loop Reservoir Management. Paper SPE 119098 presented at the SPE Reservoir Simulation Symposium, The Woodlands, Texas, USA, 2–4 February. doi: 10.2118/119098-MS.

Kraaijevanger, J.F.B.M., Egberts, P.J.P., Valstar, J.R., and Buurman, H.W. 2007. Optimal Waterflood Design Using the Adjoint Method. Paper SPE 105764 presented at the SPE Reservoir Simulation Symposium, Houston, 26–28 February. doi: 10.2118/105764-MS.

Marler, R.T. and Arora, J.S. 2004. Survey of Multi-Objective Optimization Methods for Engineering. *Structural and Multidisciplinary Optimization* **26** (6): 369–395. doi: 10.1007/s00158-003-0368-6.

Nævdal, G., Brouwer, D.R., and Jansen, J.-D. 2006. Waterflooding Using Closed-Loop Control. *Computational Geosciences* **10** (1): 37–60. doi: 10.1007/s10596-005-9010-6.

Saputelli, L., Nikolaou, M. and Economides, M.J. 2006. Real-time Reservoir Management: A Multi-Scale Adaptive Optimization and Control Approach. *Computational Geosciences* **10** (1) 61–96. doi: 10.1007/s10596-005-9011-5.

Saputelli, L., Nikolaou, M., and Economides, M.J. 2005. Self-Learning Reservoir Management. *SPE Res Eval & Eng* **8** (6): 534–547. SPE 84064-PA. doi: 10.2118/84064-PA.

Sarma, P., Aziz, K., and Durlofsky, L.J. 2005. Implementation of Adjoint Solution for Optimal Control of Smart Wells. Paper SPE 92864 presented at the SPE Reservoir Simulation Symposium, The Woodlands, Texas, USA, 31 January–2 February. doi: 10.2118/92864-MS.

Sarma, P., Durlofsky, L.J., and Aziz, K. 2008. Computational Techniques for Closed-loop Reservoir Modeling with Application to a Realistic Reservoir. *Petroleum Science and Technology* **26** (10 & 11): 1120–1140. doi: 10.1080/10916460701829580.

Srinivasan, B. Palanki, S., and Bonvin, D. 2003. Dynamic Optimization of Batch Processes: I. Characterization of the Nominal Solution. *Computers & Chemical Engineering* **27** (1): 1–26. doi: 10.1016/S0098-1354(02)00116-3.

Sudaryanto, B. and Yortsos, Y.C. 2000. Optimization of Fluid Front Dynamics in Porous Media Using Rate Control. I. Equal Mobility Fluids. *Physics of Fluids* **12** (7): 1656. doi: 10.1063/1.870417.

van Essen, G.M., Zandvliet, M.J., van den Hof, P.M.J., Bosgra, O.H., and Jansen, J.D. 2009. Robust Waterflooding Optimization of Multiple Geological Scenario. *SPE J.* **14** (1): 202–210. SPE-102913-PA. doi: 10.2118/102913-PA.

Wang, C., Li, G., and Reynolds, A.C. 2009. Production Optimization in Closed-Loop Reservoir Management. *SPE J.* **14** (3): 506–523. SPE-109805-PA. doi: 10.2118/109805-PA.

Zandvliet, M.J., Bosgra, O.H., Jasen, J.-D, van den Hof, P.M.J., and Kraaijevvanger, J.F.B.M. 2007. Bang-Bang Control and Singular Arcs in Reservoir Flooding. *J. Pet. Sci. Eng.* **58** (1–2): 186–200. doi: 10.1016/j.petrol.2006.12.008.

Zandvliet, M.J., van Doren, J.F.M., Bosgra, O.H., Jansen, J.D. and Van den Hof, P.M.J. 2008. Controllability, Observability and Identifiability in Single-Phase Porous Media Flow. *Computational Geosciences* **12** (4) 605–622. doi: 10.1007/s10596-008-9100-3.

Gijs van Essen is a PhD student at Delft University of Technology working on production optimization and reservoir management. email: g.m.vanessen@tudelft.nl. He holds an MS degree in systems and control from Delft University of Technology. **Paul Van den Hof** is professor and codirector of the Delft Center for Systems and Control. email: p.m.j.vandenhof@tudelft.nl. He holds MS and PhD degrees from the Department of Electrical Engineering, Eindhoven University of Technology. Van den Hof's research interests are in issues of system identification, parameterization, signal processing, and (robust) control design. **Jan-Dirk Jansen** is professor of reservoir systems and control at Delft University of Technology and works as a consultant for Shell International Exploration & Production. e-mail: j.d.jansen@tudelft.nl. He has worked with Shell since 1986 in research and operations in The Netherlands, Norway, and Nigeria. He holds MS and PhD degrees from Delft University of Technology.